老年精神医学講座：各論　日本老年精神医学会　131-149，2004．ワールドプランニング，東京

Antidepressant versus placebo for depressed elderly. Cochrane Database Syst Rev. 2001;(2):CD000561.

老年精神医学講座：各論　日本老年精神医学会　131-149，2004．ワールドプランニング，東京

表　うつ病による仮性痴呆と老年期痴呆の鑑別　　笠原ら 2001 を一部改変

	仮性痴呆	老年期痴呆
症状の経過	抑うつ症状→痴呆症状	痴呆症状→抑うつ症状
進行	急速	緩徐
抑うつ気分	持続的な訴え	訴えが弱く、動揺する
不安・焦燥	強い	弱い
精神運動抑制	強い	弱い
睡眠	しばしば不眠が見られる	傾眠傾向
意欲	単純な仕事も億劫がる	作業意欲はあるがまとまらない
能力低下の訴え	能力低下を強調し、深刻に悩む	能力低下を隠し、深刻味が薄い
返答	「わかりません」と答えることが多い	一生懸命考えるが、正答が少ないことが多い
社交性	回避傾向が強い	保たれていることが多い
注意力・集中力	比較的保たれている	著明に障害
見当識障害	少ない	しばしば出現

老年精神医学講座：各論　日本老年精神医学会　131-149，2004．ワールドプランニング，東京

表　抗うつ薬の副作用プロフィール　　小澤ら 2003、柿原ら 2002，塩入ら 2002 を一部改変

三環系・四環系抗うつ薬
ノルアドレナリン再取り込み阻害 振戦、頻脈、勃起障害、射精障害、血圧上昇 セロトニン再取り込み阻害 消化器症状（悪心、嘔吐） ヒスタミン H1 受容体阻害 鎮静、眠気、体重増加、低血圧 ムスカリン受容体阻害 口渇、かすみ眼、せん妄、便秘、イレウス、認知障害、尿閉 アドレナリン α1 受容体阻害 起立性低血圧、反射性頻脈、降圧剤の作用増強、めまい
SSRI
消化器症状（悪心、嘔吐）、食欲低下、頭痛、神経過敏 性機能障害、断薬症候群、セロトニン症候群、錐体外路症状 薬物相互作用による副作用 （パロキセチン）口渇、かすみ眼
SNRI
尿閉、動悸、血圧上昇、めまい、不安、異常発汗

老年精神医学講座：各論　日本老年精神医学会　131-149，2004．ワールドプランニング，東京

表　二次性躁病の原因疾患、薬剤

身体疾患
貧血
甲状腺機能亢進症
ビタミン B12 欠乏症
ナイアシン欠乏症
インフルエンザ

神経疾患
アルツハイマー病
脳血管性痴呆
脳血管障害
頭部外傷
脳炎
てんかん
多発性硬化症
正常圧水頭症
パーキンソン病
ピック病

薬剤
抗うつ薬
抗てんかん薬
ベンゾジアゼピン
メチルフェニデイト
ステロイド
L-dopa
甲状腺ホルモン

McDonald et al. 2000 を一部改変

Gender differences in brain activity generated by unpleasant word stimuli concerning body image: an fMRI study

NAOKO SHIRAO, YASUMASA OKAMOTO, TOMOYUKI MANTANI, YURI OKAMOTO and SHIGETO YAMAWAKI

Background We have previously reported that the temporomesial area, including the amygdala, is activated in women when processing unpleasant words concerning body image.

Aims To detect gender differences in brain activation during processing of these words.

Method Functional magnetic resonance imaging was used to investigate 13 men and 13 women during an emotional decision task consisting of unpleasant words concerning body image and neutral words.

Results The left medial prefrontal cortex and hippocampus were activated only among men, and the left amygdala was activated only among women during the task; activation in the apical prefrontal region was significantly greater in men than in women.

Conclusions Our data suggest that the prefrontal region is responsible for the gender differences in the processing of words concerning body image, and may also be responsible for gender differences in susceptibility to eating disorders.

Declaration of interest None. Funding detailed in Acknowledgement.

Eating disorders, which have been associated with concerns about body shape and size (American Psychiatric Association, 1994), are about 10 times more common in women than in men (Weissman & Olfson, 1995). A possible reason for this difference in susceptibility might be a gender difference in the neural processing of unpleasant information about body image. We previously reported that women showed amygdalar activation while processing unpleasant words concerning body image and perceived these words to be emotionally negative (Shirao *et al*, 2003*a*). The medial prefrontal cortex has connections to the amygdala, constituting an interaction zone between emotional and cognitive processing (Drevets & Raichle, 1998). In this study we compared the brain activation between men and women while processing these words. We predicted that the amygdala would be less activated and the medial prefrontal cortex more activated in men than in women during the emotional decision task.

METHOD

Study sample

An age-matched sample of 13 men (mean age 25.3 years, s.d.=2.8, range 21–30) and 13 women (mean age 25.2 years, s.d.=3.2, range 21–30) participated in this study (P=0.949 by two-tailed, two-sample *Student's t test*). Participants were recruited by community announcement and paid incentives equivalent to their transportation expenses. All of them were right-handed and were native Japanese speakers. Handedness was determined using the Edinburgh Handedness Inventory (Oldfield, 1971). According to self-report, participants had no history of psychiatric, neurological or other major medical illness, and had never been treated with a psychotropic medication. There was no significant difference in the average years of education between men and women: men 15.2 (s.d.=1.6) *v.* women 14.9 (s.d.=2.5); P=0.645 by two-tailed, two-sample Student's *t*-test. The average body mass index of the men was 22.4 kg/m^2 (s.d.=3.2, range 18.0–31.3) and that of the women was 21.5 kg/m^2 (s.d.=3.7, range 18.8–28.4); P=0.543 by two-tailed two-sample Student's *t*-test. The average of the total Eating Disorder Inventory – 2 (EDI–2; Garner, 1991) scores of men was 45.5 (s.d.=28.4, range 9–103) and that of women was 37.9 (s.d.=23.5, range 7–85); P=0.330 by two-tailed Wilcoxon single-rank test. The average score for the item 'body dissatisfaction' for the men was 7.43 (s.d.=5.45, range 2–19) and for the women was 11.31 (s.d.=7.00, range 0–22); P=0.330 by two-tailed Wilcoxon single-rank test. The study was conducted using a protocol approved by the ethics committee of Hiroshima University School of Medicine. All individuals provided written informed consent for participation in the study.

Emotional decision task

We used the emotional decision task developed by Tabert *et al* (2001), with some modifications. The words used in the task were selected from the database of Toglia & Battig (1978), which includes 2854 words that have been rated on several items such as familiarity and pleasantness, on a scale of 1 (very unfamiliar; very unpleasant) to 7 (very familiar; very pleasant), with 4 as the mid-point. For our study, 30 neutral words were selected from the database and translated into Japanese. We also selected 30 highly unpleasant words concerning body image, chosen from Japanese-language dictionaries and thesauri. The two groups of words did not significantly differ with regard to word length (mean length in Japanese letters: body image words 3.2, neutral words 3.1; P=0.575 by two-tailed, two-sample Student's *t*-test). Our previous validation study comparing women who had eating disorders with a control group of healthy women showed that there was no significant difference in familiarity between the two categories of words (eating disorder group mean familiarity score: body image words 4.2; neutral words 4.1, P=0.727; control group mean familiarity score: body image words 3.9, neutral words 4.1, P=0.218, by two-tailed Wilcoxon single-rank test) and there was no significant difference in the familiarity ratings of words concerning

body image between women with eating disorders and the control group (P=0.365 by two-tailed Wilcoxon single-rank test), whereas there were significant differences in pleasantness between the two categories of words (mean pleasantness score in the eating disorder group: body image words 2.4, neutral words 3.9, P=0.0002; mean pleasantness score in the control group: body image words 3.0, neutral words 4.0, P=0.0001, by two-tailed Wilcoxon single-rank test) and there were significant differences in the ratings of pleasantness between the eating disorders group and the control group (P=0.030 by two-tailed Wilcoxon single-rank test) (Shirao *et al*, 2003*b*). Both lists of words contained nouns, verbs, adjectives and adverbs.

The selected words were used to generate sets of unpleasant words concerning body image and sets of neutral words. Each word set comprised a unique combination of three words. The word sets were presented in six alternating blocks of two conditions (the task condition and the control condition) in three cycles (Fig. 1). During the task condition unpleasant word sets were presented, and during the control condition neutral word sets were presented. Each block began with a 3 s cue identifying the condition by displaying the word 'task' or 'control'. Five word sets were presented in each block. Each word set was shown for 4 s with a 1.4 s interstimulus interval (Fig. 1). The blood oxygen level-dependent (BOLD) response was recorded during three blocks of unpleasant words and three blocks of neutral words. During each interstimulus interval, a fixation cross placed centrally on the screen replaced the word set. Baseline functional magnetic resonance images were obtained during a 9 s period prior to the first block of trials, during which the individual viewed a centrally placed fixation cross. During each trial, the word set was projected to the centre of the person's field of view by a Super Video Graphics adapter computer-controlled projection system. The timing of presentation of word sets was controlled by Presentation Software Version 0.51 (Neurobehavioral Systems, Inc., San Francisco, CA, USA) and the word sets were presented in a randomised order. Immediately before functional magnetic resonance imaging (fMRI) scanning was begun, each participant was given ten practice trials (five unpleasant word sets and five neutral word sets). The words presented in the practice trials did not overlap with the experimental words.

Participants were instructed to select the most unpleasant word from each set of unpleasant words based on their personal knowledge and experience, and for each set of neutral words, participants were instructed to select the word that they thought was the most neutral; they indicated their choice by pressing one of three buttons on a response pad in the MRI scanner.

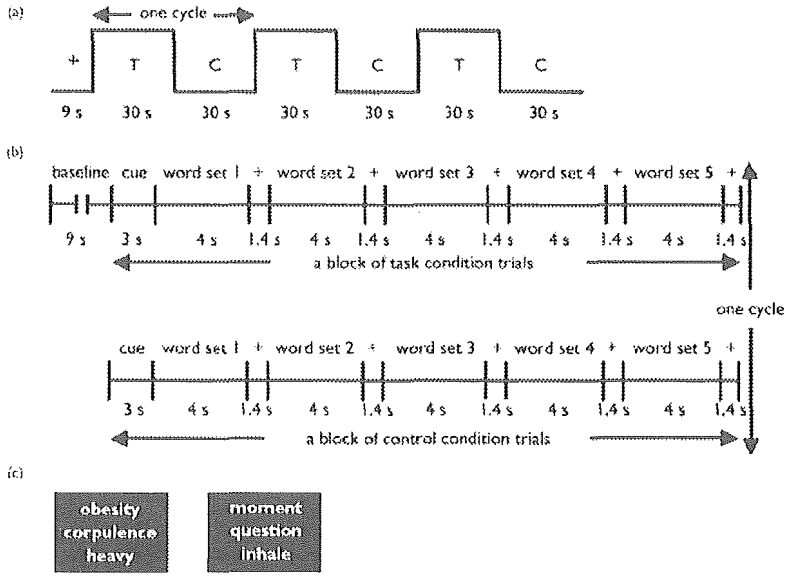

Fig. 1 Design of the study task. (a) Six alternating blocks of task condition (T) trials and control condition (C) trials were presented successively; the total scan time was 189 s (3 min and 9 s), yielding 63 images of 28 axial slices (1764 images). (b) Blocks of task condition and control condition trials were preceded by a baseline imaging period. Each block began with a cue ('task' or 'control'). The participant selected the word judged to be the most unpleasant or most neutral in each word set, by pressing one of three buttons. (C) Translations of typical word sets presented in this study (left-hand block, task condition; right-hand block, control condition).

Image acquisition and processing

The MRI scanner used was a Magnex Eclipse 1.5 T Power Drive 250 (Shimadzu Medical Systems, Kyoto, Japan). A time-course series of 63 volumes was acquired with T_2*-weighted, gradient echo, echo planar imaging (EPI) sequences. Each volume consisted of 28 slices, each 4.0 mm thick with no gap, encompassing the entire brain. The interval between two successive acquisitions of the same image (time to repetition, TR) was 3000 ms, the time to echo (TE) was 55 ms and the flip angle was 90°. The field of view was 256 mm and the matrix size 64 × 64, giving voxel dimensions of 4.0 mm × 4.0 mm × 4.0 mm. After fMRI scanning, structural scans were acquired using a T_1-weighted gradient echo pulse sequence (TR 12 ms, TE 4.5 ms, flip angle 20°, field of view 256 mm, voxel dimensions 1.0 mm × 1.0 mm × 1.0 mm), to facilitate localisation and co-registration of the functional data.

Image processing and statistical analysis were performed using Statistical Parametric Mapping (SPM) 99 software (Wellcome Department of Cognitive Neurology, London, UK) implemented in Matlab (Mathworks, Inc., Natick, MA, USA). The first two volumes of the fMRI run (pre-task period) were discarded because the magnetisation was unsteady, and the remaining 61 volumes were used for the statistical analysis. Images were corrected for motion and realigned with the first scan of the session, which served as the reference. The T_1 anatomical images were co-registered to the first functional images in each individual and aligned to a standard stereotaxic space, using the Montreal Neurological Institute (MNI) T_1 template in SPM99. The calculated non-linear transformation was applied to all functional images for spatial normalisation. Finally, the fMRI images were smoothed with a 12 mm full-width, half-maximum Gaussian filter.

Using group analysis according to a random effect model that allowed inference to the general population (Friston *et al*, 1999), we first identified brain regions that showed a significantly greater response to unpleasant word sets in comparison with the response to neutral word sets among

male and among female participants, as brain areas related to the cognition of unpleasant word stimuli concerning body image in men and women, respectively. We then took the data of 13 of the 15 women who had participated in our previous study (Shirao *et al*, 2003*a*) and directly compared the activation of the entire brain in the male and female sub-samples using the two-sample Student's *t*-test. The resulting set of voxel values for each contrast constituted an SPM{t} map. The SPM{t} maps were then interpreted by referring to the probabilistic behaviour of Gaussian random fields. The data were given an initial threshold at an uncorrected $P<0.001$ at the voxel level, and regions about which we had an *a priori* hypothesis were reported at this threshold (Elliott *et al*, 2000). For regions about which there was no clear hypothesis, a more stringent threshold of $P<0.05$ corrected at the cluster level of multiple comparison was used. The x, y and z coordinates provided by SPM, which were in MNI brain space, were converted to the x, y and z coordinates in Talairach & Tournoux's (TT) brain space (Talairach & Tournoux, 1988) using the following formulae:

(a) $x_{TT}=x_{MNI}\times 0.88-0.8$;

(b) $y_{TT}=y_{MNI}\times 0.97-3.32$;

(c) $z_{TT}=y_{MNI}\times 0.05+z_{MNI}\times 0.88-0.44$.

Labels for brain activation foci were obtained in Talairach coordinates using the Talairach Daemon software (Research Imaging Center, University of Texas, TX, USA), which provides accuracy similar to that of neuroanatomical experts (Lancaster *et al*, 2000). The labelling of areas given by this software was then confirmed by comparison with activation maps overlaid on MNI-normalised structural images.

Evaluation of pleasantness and familiarity of the word stimuli

Each participant was asked to rate the pleasantness and familiarity of all the words presented in the tasks on a scale from 1 (very unfamiliar; very unpleasant) to 7 (very familiar; very pleasant), immediately after scanning. For this rating procedure the list of words was presented in randomised order in a table format.

RESULTS

Rating of words

The ratings of familiarity with the two categories of words did not significantly differ among men (mean familiarity score: unpleasant words 3.8, neutral words 4.4, $P=0.054$ by two-tailed Wilcoxon single-rank test) or women (mean familiarity score: unpleasant words 4.3, neutral words 4.3, $P=0.456$). However, all participants rated the unpleasant words concerning body image as significantly more unpleasant than the neutral words (mean pleasantness score: unpleasant words 3.1, neutral words 4.1, $P=0.007$ in men; unpleasant words 2.7, neutral words 4.1, $P=0.002$ in women). Neither the ratings of pleasantness nor the ratings of familiarity in each word category significantly differed between the male and female groups.

Brain activation

In men there was significantly greater activation of the left hippocampus, left superior temporal gyrus, left fusiform gyrus and left medial frontal gyrus when the emotional decision task involved unpleasant words compared with neutral words, whereas the women showed significantly greater activity of the left parahippocampal gyrus including amygdala, left thalamus and right caudate body in the same comparison (Table 1, Fig. 2).

The two-sample Student's *t*-test revealed that there was a significantly higher BOLD response in the left apical prefrontal region in men than in women during the unpleasant word task compared with neutral word task (Table 1, Fig. 3). No brain area showed significantly higher activation in women than in men during any of the tasks.

Correlation between psychological data and brain activation

Among the 13 women participants, activation in the left apical prefrontal area, which was significantly lower than that in men during the unpleasant words task, was negatively correlated with the total EDI–2 score (Spearman's rank-order correlation analysis: correlational coefficient −0.699, $P=0.008$). There was no correlation between any brain area showing significant BOLD response and the EDI–2 scores or the pleasantness rating of the unpleasant words.

DISCUSSION

We used the emotional decision task to examine the brain areas engaged in the perception of unpleasant words concerning body image and to compare the patterns of brain activation in men and women. Our results showed that the left medial part of the frontal gyrus, the left limbic area excluding the amygdala, the left superior temporal gyrus and the left fusiform gyrus play an important part in processing

Table 1 Relative increases in brain activity associated with unpleasant words concerning body image (task) and neutral words (control)

	Cluster	BA	*t* score	Coordinates[1]		
				x	*y*	*z*
Men (n=13)						
Left hippocampus	696*		9.59	−32	−13	−13
Left superior temporal gyrus		21	6.54	−50	−7	−8
Left fusiform gyrus		20	6.35	−43	−25	−17
Left medial frontal gyrus	359*	9	5.71	−4	53	9
Left superior frontal gyrus		10	5.34	−15	51	18
Women (n=13)						
Left parahippocampal gyrus	404*	37	7.08	−17	−13	−15
Left thalamus	485*		6.08	−3	−11	11
Right caudate body			4.65	10	1	5
Men > women						
Left apical prefrontal region	144	9	4.36	−15	49	20

BA, Brodmann area.

1. Stereotaxic coordinates were derived from Talairach & Tournoux (1988) and refer to the medial–lateral position (x) relative to the midline (positive=right), anterior–posterior position (y) relative to the anterior commissure (positive=anterior) and superior–inferior position (z) relative to the comissural line (positive=superior).

*Areas exceeding the extent threshold of $P<0.05$ corrected at the cluster level, all other areas exceeding the height threshold of $P<0.001$ uncorrected at the cluster level and belonging to a cluster of activation with an extent of at least 140 voxels are displayed.

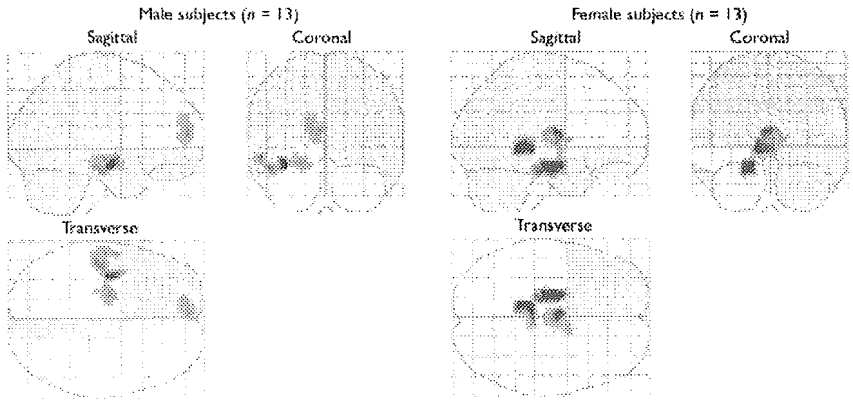

Fig. 2 Brain areas showing significantly greater activation during the task condition compared with the control condition. Three-dimensional 'look-through' projections of statistical parametric maps of the brain regions are shown (one-sample Student's *t*-test; corrected $P < 0.05$ at the cluster level; n=13; d.f.=12).

unpleasant words concerning body image in men.

Lack of amygdalar activation in men

Consistent with our hypothesis, the amygdala did not show significant activation among men; however, the gender difference of the BOLD response in the amygdala was not significant by two-sample Student's *t*-test.

The amygdala has been suggested by many studies to be strongly associated with stimuli signalling threat. Human lesion and imaging studies consistently indicate that the amygdala is concerned in fear conditioning (Morris *et al*, 1998), in the recognition of fearful facial expressions (Adolphs, 1999) and in the evocation of fearful emotional responses from direct stimulation (Halgren *et al*, 1978). The amygdala is also considered to be important in the detection of environmental threat (Scott *et al*, 1997), including verbal stimuli (Isenberg *et al*, 1999). Therefore, the lack of significant activation in the amygdala among men suggests that men may not process unpleasant words concerning body image as fearful information, whereas women seem to do so.

Medial prefrontal cortex and emotional processing

The significant activation in the medial part of the frontal gyrus – Brodmann areas (BAs) 9 and 10; medial prefrontal cortex – was only detected in men, and there was a significantly higher BOLD response in men than in women in the left apical prefrontal region (BA 9) when performing the unpleasant word task compared with the neutral word task by two-sample Student's *t*-test. These results were consistent with our hypothesis. Many previous studies have suggested that the medial prefrontal cortex might have a role generally in emotional processing. It is reported that visual stimuli that evoke emotions, such as films or pictures, activated the medial prefrontal cortex, and that recall of various emotions such as happiness, sadness and disgust, and a mixture of these emotions, all separately engaged this brain region (Lane *et al*, 1997; Reiman *et al*, 1997). Several more recent studies suggest that when people turn their attention inwards to assess self-relevant attributes or emotional awareness, activity increases in the medial prefrontal cortex (Johnson *et al*, 2002; Zysset *et al*, 2002). The medial prefrontal cortex has connections to limbic structures, including the amygdala, constituting an interaction zone between emotional processing and cognitive processing (Drevets & Raichle, 1998), and this region may have a role in modulating the emotional response in the amygdala and other limbic structures. Limbic structures, including the amygdala, are likely to respond to emotional stimuli at a sensory or perceptual level (Reiman *et al*, 1997), whereas the medial prefrontal cortex may be involved in the cognitive aspects of emotional processing, such as attention to emotion, appraisal or identification of emotion (Drevets & Raichle, 1998). From this viewpoint, the gender differences detected in our study may demonstrate differences of cognitive pattern in men and women. Our results suggest the possibility that men processed the emotional decision task including words concerning body image more cognitively rather than emotionally, and activation in the medial prefrontal cortex was prominent; on the other hand, women processed this task more emotionally rather than cognitively, and the medial prefrontal cortex did not exhibit any significant activation. Both men and women perceived the unpleasantness of the words concerning body image to the same degree, according to their subjective ratings, but the fMRI data suggest that their processes are different: women are likely to use more intuitive processing whereas men use more rational processing. This discrepancy between the genders in cognitive style related to body image may contribute to the large gender difference in susceptibility to eating disorders.

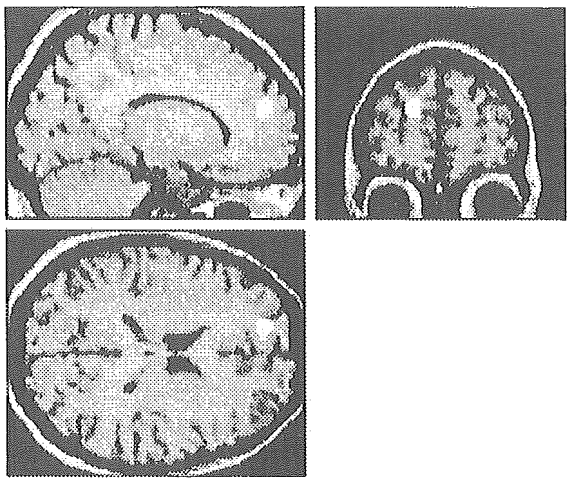

Fig. 3 Brain regions showing significantly greater activation in men than in women during the task condition of the emotional decision task compared with the control condition. Clusters of activation are overlaid onto a T_1-weighted anatomical magnetic resonance image. The white spots show areas of high activation. Two-sample Student's *t*-test; uncorrected $P < 0.001$ in height; n=26 (13 men, 13 women); d.f.=24.

Another possible explanation of the different patterns of activation in the medial prefrontal cortex between men and women may be the difference in men's familiarity with the unpleasant word set compared with the neutral words. Although the ratings of familiarity were not different between men and women (P=0.133 by Mann–Whitney U test), there was a trend for male participants to be less familiar with the unpleasant words concerning body image than with the neutral words (P=0.054 by two-tailed Wilcoxon single-rank test). When processing unfamiliar words concerning body image, men might turn more attention inwards, and subsequently the BOLD response in the medial prefrontal cortex was higher than while processing neutral words.

Among women, correlational analysis revealed that the BOLD response in the left apical prefrontal region (BA 9), which was significantly lower in women than in men, was negatively correlated with total EDI–2 scores; in other words women with higher EDI–2 scores exhibited lower activity in this brain area. These results suggest the possibility that the apical prefrontal region might be involved in the pathophysiology of eating disorders.

Comparison with other neuroimaging studies

To our knowledge, two fMRI studies concerning body image distortion have investigated the effects of pictorial body image stimuli in women with anorexia nervosa and healthy controls (Seeger *et al*, 2002; Wagner *et al*, 2003). One study reported that patients with anorexia nervosa showed activation in the right amygdala, right fusiform gyrus and brain-stem associated with stimulation with their own body image whereas healthy controls showed activation only in the fusiform gyrus (Seeger *et al*, 2002), and the other reported that patients with anorexia nervosa showed greater activation in the prefrontal cortex and the inferior parietal lobule than did controls (Wagner *et al*, 2003). The latter authors explain the discrepancy between these results as a consequence of the design of the task. Many differences in the experimental conditions between these studies and ours make it difficult to compare the brain activation data, but a possible explanation of the discrepancy between the study by Wagner *et al* (2003) and our study is the age of the participants: those in the former study were adolescents (approximately 15 years old), whereas we recruited young adults (approximately 25 years old). An fMRI study which investigated the brain activation of adult and adolescent men and women while processing emotional facial expressions reported that the adult men and adolescents (both boys and girls) showed significant activation in the bilateral orbitofrontal cortex and anterior cingulate cortex in response to an angry face, whereas the adult women showed significant activation in the left amygdala in addition to these brain areas (McClure *et al*, 2004). These results suggest that the patterns of neural responses to emotional stimuli may be different in adults and adolescents.

A positron emission tomography study of gender differences in brain activation patterns during recognition of emotional facial expressions revealed that greater amygdalar activation was observed in women and greater medial frontal activation was observed in men (Hall *et al*, 2004); these authors suggest that men might take a more analytic approach and might regulate their emotional reaction to the stimuli more than women. Although the categories of stimuli are different, these results support our findings.

Study limitations

Our study has some limitations. First, we did not administer a structured interview when selecting the participants; however, they had no psychiatric or neurological illness at the time of their participation, although we cannot rule out its occurrence in the future. Second, participants were asked to rate only the unpleasantness and familiarity of the words used. If we had also asked about the fearfulness induced by the stimuli, we might have found gender differences in subjective rating and the results with brain image data would have been more clear-cut. Last, although our data

CLINICAL IMPLICATIONS

- Gender differences in brain activation suggest differences between men and women in the style of cognition toward unpleasant stimuli concerning body image.
- This discrepancy in cognitive style may have relevance to the large gender difference in susceptibility to eating disorders.
- The medial prefrontal cortex may be the brain area linked to the pathophysiology of eating disorder.

LIMITATIONS

- We did not use a structured interview when selecting participants.
- We asked the participants to rate only pleasantness and familiarity of the word stimuli and we could find no clear relationship between brain activation and the subjective rating of the words concerning body image.
- It is unclear whether the patterns of activation in the prefrontal area were specific to the stimuli concerning body image.

NAOKO SHIRAO, MD, PhD, YASUMASA OKAMOTO, MD, PhD, TOMOYUKI MANTANI, MD, Department of Psychiatry and Neurosciences, Graduate School of Biomedical Sciences, Hiroshima University, Hiroshima, and Core Research for Evolutional Science and Technology (CREST), Japan Science and Technology Corporation, Seika; YURI OKAMOTO, MD, PhD, Hiroshima University Health Service Center, Hiroshima; SHIGETO YAMAWAKI, MD, PhD, Department of Psychiatry and Neurosciences, Graduate School of Biomedical Sciences, Hiroshima University, and CREST, Seika, Japan

Correspondence: Dr Shigeto Yamawaki, Department of Psychiatry and Neurosciences, Division of Frontier Medical Science, Programs for Biomedical Research, Graduate School of Biomedical Sciences, Hiroshima University, 1-2-3 Kasumi, Minami-ku, Hiroshima 734-8551, Japan. Tel: +81 82 257 5207; fax: +81 82 257 5209; e-mail: yamawaki@hiroshima-u.ac.jp

(First received 4 March 2004, final revision 10 August 2004, accepted 11 August 2004)

suggest that there is differential activation of the brains of men and women when processing unpleasant words concerning body image, we cannot conclude whether these results are specific to unpleasant stimuli concerning body image or would apply to a wide range of unpleasant stimuli. Among women, a lower BOLD response in the prefrontal region compared with men while processing unpleasant words concerning body image exhibited a negative correlation with the total EDI–2 score, but it is unclear whether this brain region is the focal area responsible for susceptibility to eating disorders.

In conclusion, our study revealed that the paralimbic area including the amygdala was activated only in women and that the left medial prefrontal cortex was activated only in men while performing the emotional decision task with unpleasant words concerning body image. These results suggest that gender differences in brain activation might explain the differences in the style of cognition towards unpleasant stimuli concerning body image. Further studies comparing people who have eating disorders with healthy controls and which include general unpleasant word stimuli to contrast with words specific to body image are needed to elucidate the neural substrate responsible for the onset of eating disorders.

ACKNOWLEDGEMENT

The study was supported by the Research on Psychiatric and Neurological Diseases and Mental Health, Ministry of Health, Labour and Welfare, Japan.

REFERENCES

Adolphs, R. (1999) Social cognition and the human brain. *Trends in Cognitive Science*, **3**, 469 479.

American Psychiatric Association (1994) *Diagnostic and Statistical Manual of Mental Disorders* (4th edn) (DSM IV). Washington, DC: APA.

Drevets, W. C. & Raichle, M. E. (1998) Reciprocal suppression of regional cerebral blood flow during emotional versus higher cognitive process: implications for interaction between cognition and emotion. *Cognition and Emotion*, **12**, 353 385.

Elliott, R., Friston, K. J. & Dolan, R. J. (2000) Dissociable neural responses in human reward systems. *Journal of Neuroscience*, **20**, 6159 6165.

Friston, K. J., Holmes, A. P. & Worsley, K. J. (1999) How many subjects constitute a study? *Neuroimage*, **10**, 1 5.

Garner, D. M. (1991) *Eating Disorder Inventory 2 (EDI 2)*. Odessa, FL: Psychological Assessment Resources.

Halgren, E., Walter, R. D., Cherlow, D. G., et al (1978) Mental phenomena evoked by electrical stimulation of the human hippocampal formation and amygdala. *Brain*, **101**, 83 117.

Hall, G. B., Witelson, S. F., Szechtman, H., et al (2004) Sex differences in functional activation patterns revealed by increased emotion processing demands. *Neuroreport*, **15**, 219 223.

Isenberg, N., Silbersweig, D., Engelien, A., et al (1999) Linguistic threat activates the human amygdala. *Proceedings of the National Academy of Science USA*, **96**, 10456 10459.

Johnson, S. C., Baxter, L. C., Wilder, L. S., et al (2002) Neural correlates of self-reflection. *Brain*, **125**, 1808 1814.

Lancaster, J. L., Woldorff, M. G., Parsons, L. M., et al (2000) Automated Talairach atlas labels for functional brain mapping. *Human Brain Mapping*, **10**, 120 131.

Lane, R. D., Reiman, E. M., Bradley, M. M., et al (1997) Neuroanatomical correlates of pleasant and unpleasant emotion. *Neuropsychologia*, **35**, 1437 1444.

McClure, E. B., Monk, C. S., Nelson, E. E., et al (2004) A developmental examination of gender differences in brain engagement during evaluation of threat. *Biological Psychiatry*, **55**, 1047 1055.

Morris, J. S., Ohman, A. & Dolan, R. J. (1998) Conscious and unconscious emotional learning in the human amygdala. *Nature*, **393**, 467 470.

Oldfield, R. C. (1971) The assessment and analysis of handedness: the Edinburgh inventory. *Neuropsychologia*, **9**, 97 113.

Reiman, E. M., Lane, R. D., Ahern, G. L., et al (1997) Neuroanatomical correlates of externally and internally generated human emotion. *American Journal of Psychiatry*, **154**, 918 925.

Scott, S. K., Young, A. W., Calder, A. J., et al (1997) Impaired auditory recognition of fear and anger following bilateral amygdala lesions. *Nature*, **385**, 254 257.

Seeger, G., Braus, D. F., Ruf, M., et al (2002) Body image distortion reveals amygdala activation in patients with anorexia nervosa a functional magnetic resonance imaging study. *Neuroscience Letters*, **326**, 25 28.

Shirao, N., Okamoto, Y., Okada, G., et al (2003a) Temporomesial activation in young females associated with unpleasant words concerning body image. *Neuropsychobiology*, **48**, 136 142.

Shirao, N., Okamoto, Y., Okamoto, Y., et al (2003b) Ratings of negative body image words, negative emotion words and neutral words by eating disorder patients and healthy subjects. *Brain Sciences and Mental Disorders*, **15**, 141 147.

Tabert, M. H., Borod, J. C., Tang, C. Y., et al (2001) Differential amygdala activation during emotional decision and recognition memory tasks using unpleasant words: an fMRI study. *Neuropsychologia*, **39**, 556 573.

Talairach, J. & Tournoux, P. (1988) *Co-planar Stereotaxic Atlas of the Human Brain*. Stuttgart: Thieme.

Toglia, M. P. & Battig, W. F. (1978) *Handbook of Semantic Word Norms*. Hillsdale, NJ: Lawrence Erlbaum.

Wagner, A., Ruf, M., Braus, D. F., et al (2003) Neuronal activity changes and body image distortion in anorexia nervosa. *Neuroreport*, **14**, 2193 2197.

Weissman, M. M. & Olfson, M. (1995) Depression in women: implications for health care research. *Science*, **269**, 799 801.

Zysset, S., Huber, O., Ferstl, E., et al (2002) The anterior frontomedian cortex and evaluative judgment: an fMRI study. *Neuroimage*, **15**, 983 991.

nature neuroscience

Prediction of immediate and future rewards differentially recruits cortico-basal ganglia loops

Saori C Tanaka[1–3], Kenji Doya[1–3], Go Okada[3,4], Kazutaka Ueda[3,4], Yasumasa Okamoto[3,4] & Shigeto Yamawaki[3,4]

Evaluation of both immediate and future outcomes of one's actions is a critical requirement for intelligent behavior. Using functional magnetic resonance imaging (fMRI), we investigated brain mechanisms for reward prediction at different time scales in a Markov decision task. When human subjects learned actions on the basis of immediate rewards, significant activity was seen in the lateral orbitofrontal cortex and the striatum. When subjects learned to act in order to obtain large future rewards while incurring small immediate losses, the dorsolateral prefrontal cortex, inferior parietal cortex, dorsal raphe nucleus and cerebellum were also activated. Computational model–based regression analysis using the predicted future rewards and prediction errors estimated from subjects' performance data revealed graded maps of time scale within the insula and the striatum: ventroanterior regions were involved in predicting immediate rewards and dorsoposterior regions were involved in predicting future rewards. These results suggest differential involvement of the cortico-basal ganglia loops in reward prediction at different time scales.

In daily life, people make decisions based on the prediction of rewards at different time scales; for example, one might do daily exercise to achieve a future fitness goal, or resist the temptation of sweets to avoid future weight gain. Damage to the prefrontal cortex often impairs daily decision making, which requires assessment of future outcomes[1,2]. Lesions in the core of the nucleus accumbens in rats result in a tendency to choose small immediate rewards over larger future rewards[3]. Low activity of the central serotonergic system is associated with impulsive behavior in humans[4], and animals with lesions in the ascending serotonergic pathway tend to choose small immediate rewards over larger future rewards[5,6]. A possible mechanism underlying these observations is that different sub-loops of the topographically organized cortico-basal ganglia network are specialized for reward prediction at different time scales and that they are differentially activated by the ascending serotonergic system[7]. To test whether there are distinct neural pathways for reward prediction at different time scales, we developed a 'Markov decision task' in which an action affects not only the immediate reward but also future states and rewards. Using fMRI, we analyzed brain activity in human subjects as they performed this task. Recent functional brain imaging studies have shown the involvement of specific brain areas, such as the orbitofrontal cortex (OFC) and the ventral striatum, in prediction and perception of rewards[8–11]. In these previous studies, however, rewards were given either independent of the subject's actions or as a function of the current action. Our Markov decision task probes decision making in a dynamic context, with small losses followed by a large positive reward. The results of the block-design analysis suggest differential involvement of brain areas in decision making by prediction of rewards at different time scales. By analyzing subjects' performance data according to a theoretical model of reinforcement learning, we found a gradient of activation within the insula and the striatum for prediction of rewards at different time scales.

RESULTS

Behavioral results

In the Markov decision task, a visual signal (one of three shapes) was presented at the start of each trial to indicate one of three states, and the subject selected one of two actions: pressing the right or left button with the right hand (Fig. 1a; see Methods for details). For each state, the subject's action choice affected not only the immediate reward, but also the state subsequently presented (Fig. 1b,c).

The rule of state transition was fixed during the entire experiment (Fig. 1), but the rules of reward delivery changed according to the task condition. In the SHORT condition, action a_1 gives a small positive reward ($+r_1 = 20$ yen average; see Methods) and action a_2 gives a small loss ($-r_1$) in all three states (Fig. 1b). The optimal behavior for maximizing total reward in the SHORT condition is to collect small positive rewards by taking action a_1 at each state. In the LONG condition, action a_2 at state s_3 gives a big bonus ($+r_2 = 100$ yen average; see Methods), and action a_1 at state s_1 results in a big loss ($-r_2$; Fig. 1c). The optimal behavior is to receive small losses at state s_1 and s_2 to obtain a large positive reward at state s_3 by taking action a_2 at each state; this is opposite to the optimal behavior in the SHORT condition. Whereas the optimal strategy in the SHORT condition results in small, immediate rewards at each step, the optimal strategy in the LONG condition results in small immediate losses but a net positive reward by the end of one cycle. Thus, for successful action in the LONG condition, subjects must consider both the

[1]Department of Bioinformatics and Genomics, Nara Institute of Science and Technology, 8916-5 Takayama, Ikoma, Nara 630-0101, Japan. [2]Department of Computational Neurobiology, ATR Computational Neuroscience Laboratories, 2-2-2 Hikaridai, Keihanna Science City, Kyoto 619-0288, Japan. [3]CREST, Japan Science and Technology Agency, 2-2-2 Hikaridai, Keihanna Science City, Kyoto 619-0288, Japan. [4]Department of Psychiatry and Neurosciences, Hiroshima University, 1-2-3 Kasumi, Minamiku, Hiroshima 734-8551, Japan. Correspondence should be addressed to K.D. (doya@atr.jp).

Published online 4 July 2004; doi:10.1038/nn1279

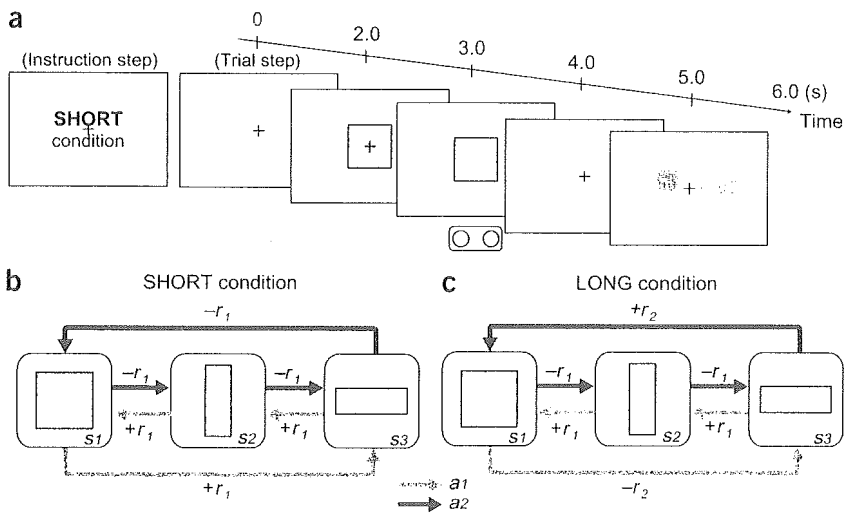

Figure 1 Experimental design. (**a**) Sequences of stimulus and response events in the task. At the beginning of each condition block, the condition is informed by displaying text (6 s), such as 'SHORT condition' (instruction step). In each trial step, a fixation point is presented on the screen, and after 2 s, one of three shapes (square, vertical rectangle or horizontal rectangle) is presented for 1 s. As the fixation point vanishes after 1 s, the subject presses either the right or left button within 1 s. After a short delay (1 s), a reward for that action is presented by a number (indicating yen gained or lost) and the past cumulative reward is shown by a bar graph. Thus, one trial step takes 6 s. (**b**,**c**) The rules of the reward and state transition for action a_1 (magenta arrows) and action a_2 (blue arrows) in the SHORT (**b**) and LONG (**c**) conditions. The small reward r_1 was 10, 20 or 30 yen, with equal probability, and the large reward r_2 was 90, 100, or 110 yen. The rule of state transition was the same for all conditions: $s_3 \rightarrow s_2 \rightarrow s_1 \rightarrow s_3 \ldots$ for action a_1, and $s_1 \rightarrow s_2 \rightarrow s_3 \rightarrow s_1 \rightarrow \ldots$ for action a_2. Although the optimal behaviors are opposite (SHORT: a_1; LONG: a_2), the expected cumulative reward during one cycle of the optimal behavior is 60 yen in both the SHORT ($+20 \times 3$) and LONG (-20, -20, $+100$) conditions.

immediate reward and the future reward expected from the subsequent state, and for success in the SHORT condition, subjects need to consider only the immediate outcome of their actions. Subjects performed 15 trials in a SHORT condition block and 15 trials in a LONG condition block. There were also two control conditions, NO (reward was always zero) and RANDOM (reward was $+r_1$ or $-r_1$, regardless of state or action), so a total of four condition blocks were performed (see Fig. 2a for task schedule).

All subjects successfully learned the optimal behaviors: taking action a_1 in the SHORT condition (Fig. 2b) and action a_2 in the LONG condition (Fig. 2c). Cumulative rewards within each SHORT block (Fig. 2d) and LONG block (Fig. 2e) also indicate successful learning. It can be seen from the single-subject data in the LONG condition (Fig. 2e, orange) that the subject learned to lose small amounts ($-r_1$) twice to get a big bonus ($+r_2$). The average cumulative reward in the last block was 254 yen in the SHORT condition and 257 yen in the LONG condition, which was 84.7% and 85.7%, respectively, of the theoretical optimum of 300 yen.

Block-design analysis

To find the brain areas that are involved in immediate reward prediction, we compared brain activity during the SHORT condition and the NO condition, in which reward was always zero. In the SHORT versus NO contrast, a significant increase in activity was observed in the lateral OFC (Fig. 3a), the insula and the occipitotemporal area (OTA) (Fig. 3b), as well as in the striatum, the globus pallidus (GP) (Fig. 3c) and the medial cerebellum (Fig. 3d) (threshold of $P < 0.001$, uncorrected for multiple comparisons). These areas may be involved in reward prediction based on immediate outcome.

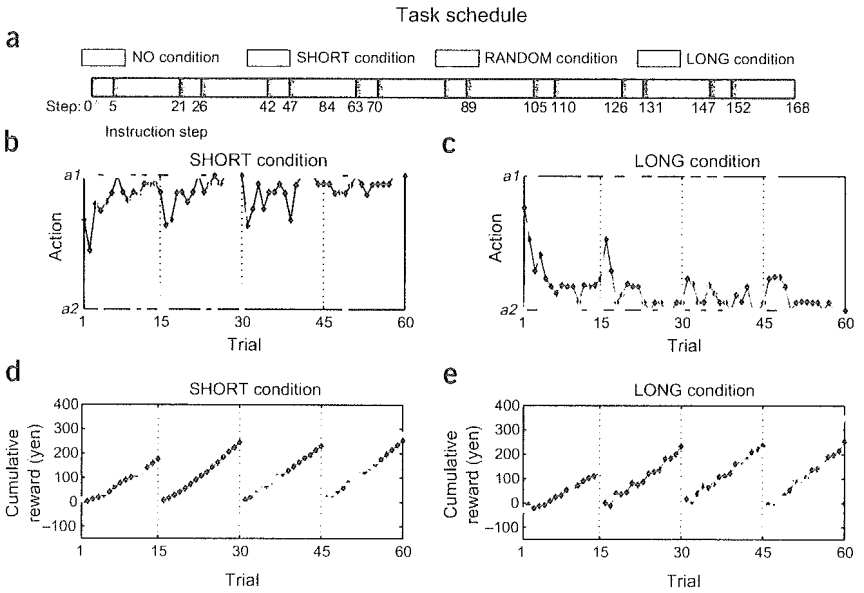

Figure 2 Task schedule and behavioral results. (**a**) A set of four condition blocks—NO (4 trials), SHORT (15 trials), RANDOM (4 trials), LONG (15 trials)—was repeated four times. At the beginning of each condition block, the task condition was presented to the subject (instruction step); thus, the entire experiment consisted of 168 steps (152 trial steps and 16 instruction steps). (**b**,**c**) The selected action of a representative single subject (orange) and the group average ratio of selecting a_1 (blue) in the (**b**) SHORT and (**c**) LONG conditions. (**d**,**e**) The accumulated reward in each block of a representative single subject (orange) and the group average (blue) in the (**d**) SHORT and (**e**) LONG conditions. To clearly show the learning effects, data from four trial blocks in the SHORT and LONG conditions are concatenated, with the dotted lines indicating the end of each condition block.

To identify areas involved in future reward prediction, we compared the brain activity during LONG and SHORT conditions. In the LONG versus SHORT contrast, a robust increase in activity was observed in the ventrolateral prefrontal cortex (VLPFC), the insula, the dorsolateral prefrontal cortex (DLPFC), the dorsal premotor cortex (PMd), the inferior parietal cortex (IPC) (Fig. 4a), the striatum, GP (Fig. 4b), the dorsal raphe nucleus (Fig. 4c), the lateral cerebellum (Fig. 4d), the posterior cingulate cortex and the subthalamic nucleus ($P < 0.001$, uncorrected). Activity in the striatum was highly significant (threshold at $P < 0.05$, corrected for a small volume when using an anatomically defined region of interest (ROI) in the striatum; see Methods). These areas are specifically involved in decision making based on the prediction of reward in multiple steps in the future. In the LONG versus NO contrast, the activated areas were approximately the union of the areas activated in the SHORT versus NO and LONG versus SHORT contrasts. These results were consistent with our expectation that both immediate and future reward prediction were required in the LONG condition. The results of block-design analysis, including the LONG versus NO contrast, are summarized in Supplementary Table 1 online. Activitions in both SHORT and LONG conditions were stronger in the first two blocks, when subjects were involved in active trial and error, than in the last two blocks when the subjects' behavior became repetitive.

We compared the activitions in the SHORT versus NO contrast and the LONG versus SHORT contrast, and observed that three regions showed significant activity in both contrasts: the lateral prefrontal cortex (lateral OFC and VLPFC), the insula and the anterior striatum (Fig. 5). In the lateral PFC (Fig. 5a), although the activities in lateral OFC for the SHORT versus NO contrast (red) and in the VLPFC for the LONG versus SHORT contrast (blue) were close in location, they were clearly separated on the cortical surface. Activities in the insula were also separated (Fig. 5b). In the anterior striatum (Fig. 5c), we found limited overlaps between the two contrasts (green). In all three areas, activations in the SHORT versus NO contrast were found in the ventral parts, whereas activations in the LONG versus SHORT contrast were found in the dorsal parts.

These results of block-design analysis suggest differential involvement of brain areas in predicting immediate and future rewards.

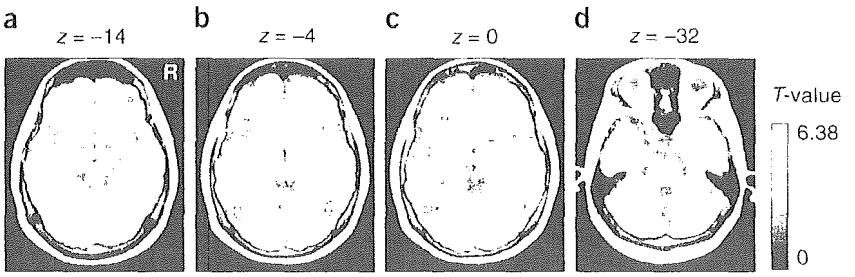

Figure 3 Brain areas activated in the SHORT versus NO contrast ($P < 0.001$, uncorrected; extent threshold of four voxels). (**a**) Lateral OFC. (**b**) Insula. (**c**) Striatum. (**d**) Medial cerebellum.

Performance-based multiple regression analysis

To further clarify the brain structures specific to reward prediction at different time scales, we estimated how much reward the subjects should have predicted on the basis of their performance data and used their time courses as the explanatory variables of regression analysis. We took the theoretical framework of temporal difference (TD) learning[12], which has been successfully used for explaining reward-predictive activations of the midbrain dopaminergic system as well as those of the cortex and the striatum[8,11,13–16]. In TD learning theory, the predicted amount of future reward starting from a state $s(t)$ is formulated as the 'value function'

$$V(t) = E[r(t+1) + \gamma r(t+2) + \gamma^2 r(t+3) + \ldots]. \quad (1)$$

Any deviation from the prediction is given by the TD error

$$\delta(t) = r(t) + \gamma V(t) - V(t-1), \quad (2)$$

which is a crucial learning signal for reward prediction and action selection. The 'discount factor' γ ($0 \leq \gamma < 1$) controls the time scale of prediction: when $\gamma = 0$, only the immediate reward $r(t+1)$ is considered, but as γ approaches 1, rewards in the further future are taken into account.

We estimated the time courses of reward prediction $V(t)$ and prediction error $\delta(t)$ from each subject's performance data and used them as the explanatory variables in multiple regression analysis with fMRI data (see Methods). In our Markov decision task, the minimum value of γ needed to find the optimal action in the LONG condition is 0.36, and any small value of γ is sufficient in the SHORT condition. From the results of our block-design analysis, we assumed that different networks involving the cortex and basal ganglia are specialized for reward prediction at different time scales and that they work in parallel, depending on the requirement of the task. Thus, we varied the discount factor γ as 0, 0.3, 0.6, 0.8, 0.9 and 0.99: small γ for immediate reward prediction and large γ for long future reward prediction. An example of these time courses is shown in Supplementary Figure 1 online.

We observed a significant correlation with reward prediction $V(t)$ in the medial prefrontal cortex (mPFC; including the anterior cingulate cortex (ACC) and the medial OFC) (Fig. 6a) and bilateral insula (Fig. 6b), left hippocampus and left temporal pole ($P < 0.001$, uncorrected; see Supplementary Table 2 online). Figure 6 shows the correlated

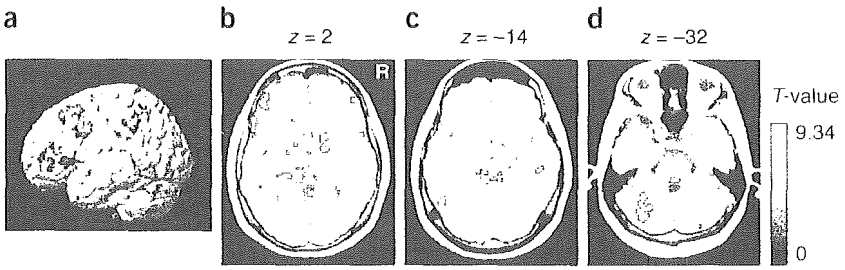

Figure 4 Brain areas activated in the LONG versus SHORT contrast ($P < 0.0001$, uncorrected; extent threshold of four voxels for illustration purposes). (**a**) DLPFC, IPC, PMd. (**b**) GP, striatum. (**c**) Dorsal raphe nucleus. (**d**) Left lateral cerebellum.

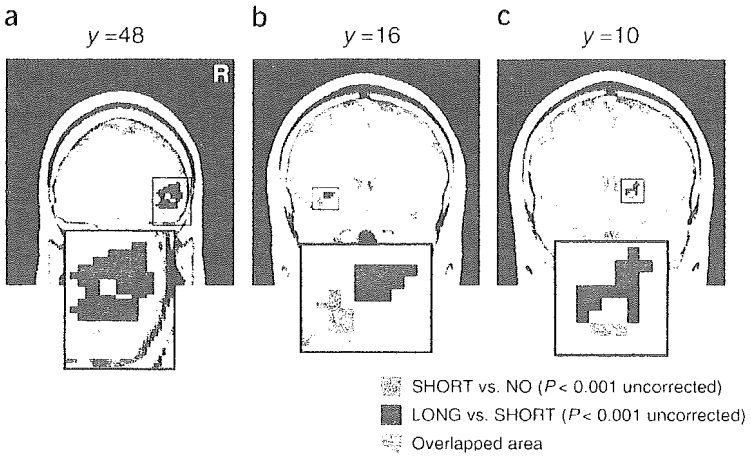

Figure 5 Comparison of brain areas activated in the SHORT versus NO contrast (red) and the LONG versus SHORT contrast (blue). (**a–c**) These figures show activation maps focused on (**a**) the lateral OFC (red (*x*, *y*, *z*) = (38, 46, −14); blue (46, 47, 3)) (**b**) the insula (red (−36, 13, −4); blue (−30, 18, 1)), and (**c**) the striatum (red (18, 10, 0); blue (18, 12, 3)) where we observed significant activation in both contrasts. The areas where activity overlapped area are shown in green.

voxels within these areas using a gradient of colors for different γ values (red for $\gamma = 0$, blue for $\gamma = 0.99$). Activity in the mPFC, temporal pole and hippocampus correlated with reward prediction with a longer time scale ($\gamma \geq 0.6$). Furthermore, in the insula, we found a graded map of activity for reward prediction at different time scales (Fig. 6b). Whereas activity in the ventroanterior region correlated with reward prediction at a shorter time scale, activity in the dorsoposterior region correlated with reward prediction at a longer time scale.

We also found, in the basal ganglia, significant correlation with reward prediction error $\delta(t)$ using a wide range of time scales (Fig. 6c; $P < 0.001$, uncorrected; see **Supplementary Table 3** online and Methods). Again, we found a graded map, which had a short time scale in the ventroanterior part and a long time scale in the dorsoposterior part. The coincidence of the ventroanterior-dorsoposterior maps and the ventroanterior-dorsoposterior shifts in activities (Fig. 6b,c) indicate that, while the ventroanterior regions with smaller γ were predominantly active in the SHORT condition, the dorsoposterior regions with larger γ became more active in the LONG condition.

DISCUSSION

The results of the block-design and performance-based regression analyses suggest differential involvement of brain areas in action learning by prediction of rewards at different time scales. Both block-design and performance-based regression analyses showed activity in the insula and the anterior striatum. Activations of the ventral region in the SHORT versus NO contrast and the dorsal region in the LONG versus SHORT contrast in each area (Fig. 5) are consistent with the ventroanterior-dorsoposterior maps of the discount factor γ found in performance-based regression analysis (Fig. 6).

The insula takes a pivotal position in reward processing by receiving primary taste and visceral sensory input[17] and sending output to the OFC[18] and the striatum[19]. Previous studies showed that the insula is activated with anticipation of primary reward[10] and that insular lesion causes deficits in incentive learning for primary reward[20]. Our results confirm the role of the insula in prediction of non-primary, monetary reward[21], and further suggest heterogeneous organization within the insula. Previous imaging studies also showed involvement of the insula, especially the ventroanterior region, in processing aversive outcomes[22,23]. Thus a possible interpretation of the activation of the insula in the LONG condition is that it

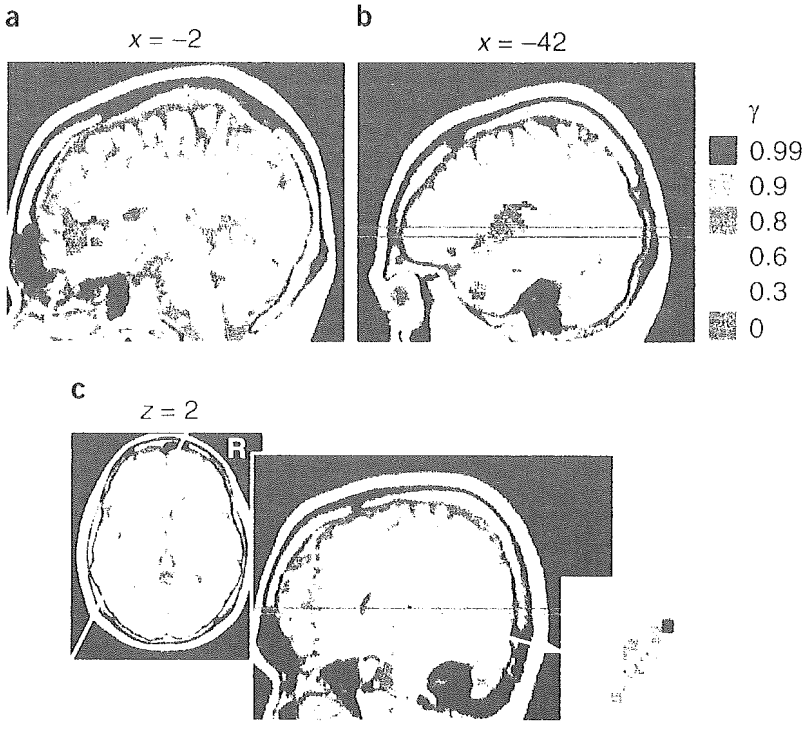

Figure 6 Voxels with a significant correlation (height threshold $P < 0.001$, uncorrected; extent threshold of four voxels) with reward prediction $V(t)$ and prediction error $\delta(t)$ are shown in different colors for different settings of the discount factor γ. Voxels correlated with two or more regressors are shown by a mosaic of colors. (**a**, **b**) Significant correlation with reward prediction $V(t)$. (**a**) mPFC. (**b**) Insula. (**c**) Significant correlation with reward prediction error $\delta(t)$ restricted to ROI in the striatum (slice at white line in horizontal slice at $z = 2$ mm). Note the ventroanterior-to-dorsoposterior gradient with the increase in γ both in the insula and the striatum. Red and blue lines correspond to the *z*-coordinate levels of activation peaks in the insula and striatum shown in **Figure 5b,c** (red for the SHORT versus NO and blue for the LONG versus SHORT contrasts).

reflected the losses that subjects acquired before getting a large reward. However, we also ran a regression analysis using losses and found significant correlation in the ventroanterior region of the insula. Anatomical and physiological studies of the insula also showed involvement of its ventroanterior part in perception of aversive stimuli[17]. Thus we argue that the activation of dorsoposterior insula is not simply due to losses in the LONG condition.

Previous brain imaging and neural recording studies suggest a role for the striatum in prediction and processing of reward[9,10,14,21,24–29]. Consistent with previous fMRI studies[8,11,16], our results showed striatal activity correlated with the error of reward prediction. Reinforcement learning models of the basal ganglia[13–15] posit that the striatum learns reward prediction and action selection based on the reward prediction error $\delta(t)$ represented by the dopaminergic input. Correlation of striatal activity with reward prediction error $\delta(t)$ could be due to dopamine-dependent plasticity of cortico-striatal synapses[30].

In lateral OFC, DLPFC, PMd, IPC and dorsal raphe, we found significant activations in the block-design analyses, but we did not find strong correlation in regression analyses. This may be because these areas perform functions that are helpful for reward prediction and action selection, but their activities do not directly represent the amount of predicted reward or prediction error at a specific time scale.

In reinforcement learning theory, an optimal action selection is realized by taking the action a that maximizes the 'action value' $Q(s, a)$ at a given state s. The action value is defined as $Q(s, a) = E[\, r(s, a) + \gamma V(s'(s, a))]$ and represents the expected sum of the immediate reward $r(s, a)$ and the weighted future rewards $V(s'(s, a))$, where $s'(s, a)$ means the next state reached by taking an action a at a state s (refs. 12,15). According to this framework, we can see that prediction of immediate reward $r(s, a)$ is helpful for action selection based on rewards at either short or long time scales, that is, with any value of the discount factor γ. On the other hand, prediction of state transition $s'(s, a)$ is helpful only in long-term reward prediction with positive values of γ.

In the lateral OFC, we observed significant activity in both the SHORT versus NO and the LONG versus NO contrasts (**Supplementary Table 1** online), but no significant correlation with reward prediction $V(t)$ or reward prediction error $\delta(t)$ in regression analysis. This suggests that the lateral OFC takes the role of predicting immediate reward $r(s, a)$, which is used for action selection in both SHORT and LONG conditions, but not in the NO condition. This interpretation is consistent with previous studies demonstrating the OFC's role in prediction of rewards, immediately following sensorimotor events[31,32], and action selection based on reward prediction[23,33,34].

In the DLPFC, PMd and IPC, there were significant activations in both the LONG versus NO and the LONG versus SHORT contrasts (**Supplementary Table 1** online) but no significant correlation with either $V(t)$ or $\delta(t)$. A possible interpretation is that this area is involved in prediction of future state $s'(s, a)$ in the LONG condition but not in the SHORT or NO conditions. This interpretation is consistent with previous studies showing the role of these cortical areas in imagery[35], working memory and planning[36,37].

The dorsal raphe nucleus was activated in the LONG versus SHORT contrast, but was not correlated with $V(t)$ or $\delta(t)$. In consideration of its serotonergic projection to the cortex and the striatum and serotonin's implication with behavioral impulsivity[4–6], a possible role for the dorsal raphe nucleus is to control the effective time scale of reward prediction[7]. Its higher activity in the LONG condition, where a large setting of γ is necessary, is consistent with this hypothesis.

Let us consider the present experimental results in light of the anatomy of cortico-basal ganglia loops (illustrated in **Supplementary Fig. 2**). The cortex and the basal ganglia both have parallel loop organization, with four major loops (limbic, cognitive, motor and oculomotor) and finer, topographic sub-loops within each major loop[38]. Our results suggest that the areas within the limbic loop[39], namely the lateral OFC and ventral striatum, are involved in immediate reward prediction. On the other hand, areas within the cognitive and motor loops[38], including the DLPFC, IPC, PMd and dorsal striatum, are involved in future reward prediction. The connections from the insula to the striatum are topographically organized, with the ventral-anterior, agranular cortex projecting to the ventral striatum and the dorsal-posterior, granular cortex projecting to the dorsal striatum[19] (see **Supplementary Fig. 2**). The graded maps shown in **Figure 6b,c** are consistent with this topographic cortico-striatal organization and suggest that areas that project to the more dorsoposterior part of the striatum are involved in reward prediction at a longer time scale. These results are consistent with the observations that localized damages within the limbic and cognitive loops manifest as deficits in evaluation of future rewards[1,3,34,40,41] and learning of multi-step behaviors[42]. The parallel learning mechanisms in the cortico-basal ganglia loops used for reward prediction at a variety of time scales may have the merit of enabling flexible selection of a relevant time scale appropriate for the task and the environment at the time of decision making.

A possible mechanism for selection or weighting of different cortico-basal ganglia loops with an appropriate time scale is serotonergic projection from the dorsal raphe nucleus[7] (see **Supplementary Fig. 2**), which was activated in the LONG versus SHORT contrast. Although serotonergic projection is supposed to be diffuse and global, differential expression of serotonergic receptors in the cortical areas and in the ventral and dorsal striatum[43,44] would result in differential modulation. The mPFC, which had significant correlation with reward prediction $V(t)$ at long time scales ($\gamma \geq 0.6$), may regulate the activity of the raphe nucleus through reciprocal connection[45,46]. This interpretation is consistent with previous studies using tasks that require long-range prospects for problem solving, such as the gambling problem[1] or delayed reward task[2], which showed involvement of the medial OFC. Future studies using the Markov decision task under pharmacological manipulation of the serotonergic system should clarify the role of serotonin in regulating the time scale of reward prediction.

Recent brain imaging and neural recording studies report involvement of a variety of cortical areas and the striatum in reward processing[8–11,16,21,23–29,32,33,47–49]. Although some neural recording studies have used experimental tasks that require multiple trial steps for getting rewards[47,48], none of the previous functional brain imaging studies addressed the issue of reward prediction at different time scales, and considered only rewards immediately following stimuli or actions. We were able extract specific functions of OFC, DLPFC, mPFC, insula and cortico-basal ganglia loops using our new Markov decision task and a reinforcement learning model–based regression analysis. Our regression analysis not only extracted brain activities specific to reward prediction, but also revealed a topographic organization in reward prediction (**Fig. 6**). The combination of our Markov decision task with event-related fMRI and magnetoencephalography (MEG) should further clarify the functions used for reward prediction and perception at different time scales, and at finer spatial and temporal resolutions.

METHODS

Subjects. Twenty healthy, right-handed volunteers (18 males and 2 females, ages 22–34 years) gave informed consent to participate in the experiment, which was conducted with the approval of the ethics and safety committees of Advanced Telecommunication Research Institute International (ATR) and Hiroshima University.

Behavioral task. In the Markov decision task (**Fig. 1**), one of three states was visually presented to the subject using three different shapes, and the subject selected one of two actions by pressing one of two buttons using their right hand (**Fig. 1a**). The rule of state transition was the same for all conditions: $s_3 \rightarrow s_2 \rightarrow s_1 \rightarrow s_3 \ldots$ for action a_1, and $s_1 \rightarrow s_2 \rightarrow s_3 \rightarrow s_1 \rightarrow \ldots$ for action a_2. The rules for reward, however, changed in each condition. In the SHORT condition (**Fig. 1b**), action a_1 results in a small positive reward ($+r_1$ = 10, 20 or 30 yen, with equal probabilities), whereas action a_2 results in a small loss ($-r_1$) at any of the three states. Thus, the optimal behavior is to collect small positive rewards at each state by performing action a_1. In the LONG condition (**Fig. 1c**), however, the reward setting is such that action a_2 gives a large positive reward ($+r_2$ = 90, 100 or 110 yen) at state s_3, and action a_1 gives a large loss ($-r_2$) at state s_1. Thus, the optimal behavior is to receive small losses at states s_1 and s_2 to obtain a large positive reward at state s_3 by taking action a_2 at each state. There were two control conditions: the NO condition, where the reward was always zero, and the RANDOM condition, where the reward was positive ($+r_1$) or negative ($-r_1$) with equal probability, regardless of state or action.

Subjects completed 4 trials in a NO condition block, 15 trials in a SHORT condition block, 4 trials in a RANDOM condition block and 15 trials in a LONG condition block. A set of four condition blocks (NO, SHORT, RANDOM, LONG) was repeated four times (**Fig. 2a**). Subjects were informed of the current condition at the beginning of each condition block by text on the screen (first slide in **Fig. 1a**); thus, the entire experiment consisted of 168 steps (152 trial steps and 16 instruction steps), taking about 17 min. The mappings of the three states to the three figures, and the two buttons to the two actions, were randomly set at the beginning of each experiment, so that subjects were required to learn the amount of reward associated with each figure-button pair in both SHORT and LONG conditions. Furthermore, in the LONG condition, subjects had to learn the subsequent figure for each figure-action pair and take into account the amount of reward expected from the subsequent figure in selecting a button.

fMRI imaging. A 1.5-tesla scanner (Shimadzu-Marconi, Magnex Eclipse) was used to acquire both structural T1-weighted images (repetition time, TR = 12 ms, TE = 4.5 ms, flip angle = 20°, matrix = 256 × 256, FoV = 256 mm, thickness = 1 mm, slice ga$P$ = 0 mm) and T2*-weighted echo planar images (TR = 6 s, TE = 55 ms, flip angle = 90°, 50 transverse slices, matrix = 64 × 64, FoV = 192 mm, thickness = 3 mm, slice gap = 0 mm) showing blood oxygen level–dependent (BOLD) contrasts.

Because the aim of the present study was to identify brain activity underlying reward prediction over multiple trial steps, we acquired functional images every 6 s (TR = 6 s), in synchrony with single trials. Although shorter TRs and event-related designs are often used in experiments that aim to distinguish brain responses to events within a trial[9,11,21,26], analysis of those finer events in time were not the focus of the current study. With this longer TR, the BOLD signal in a single scan contained a mixture of responses for a reward-predictive stimulus and reward feedback. However, because of the progress of learning and the stochastic nature of the amount of reward, the time courses of reward prediction $V(t)$ and prediction error $\delta(t)$ over the 168 trial steps were markedly different. Thus, we could separate activity corresponding to reward prediction from that corresponding to outcomes by using both reward prediction $V(t)$ and reward outcome $r(t)$ in multiple regression analysis, as described below.

Data analysis. The data were pre-processed and analyzed with SPM99 (www.fil.ion.ucl.ac.uk/spm/spm99.html). The first two volumes of images were discarded to avoid T1 equilibrium effects. The images were realigned to the first image as a reference, spatially normalized with respect to the Montreal Neurological Institute EPI template, and spatially smoothed with a Gaussian kernel (8 mm, full-width at half-maximum).

We conducted two types of analysis. One was block-design analysis using four boxcar regressors covering the whole experiment, convolved with a hemodynamic response function as the reference waveform for each condition (NO, SHORT, RANDOM, LONG). We did not find substantial differences between SHORT versus NO and SHORT versus RANDOM contrasts, or between LONG versus NO and LONG versus RANDOM contrasts. Therefore we report here only the results with the NO condition as the control condition. The other method was multivariate regression analysis using explanatory variables, representing the time course of the reward prediction $V(t)$ or reward prediction error $\delta(t)$ at six different timescales γ, estimated from subjects' performance data (described below).

In both analyses, images of parameter estimates for the contrast of interest were created for each subject. These were then entered into a second-level group analysis using a one-sample t test at a threshold of $P < 0.001$, uncorrected for multiple comparisons (random effects analysis) and extent threshold of four voxels. Small-volume correction (SVC) was done at a threshold of $P < 0.05$ using an ROI within the striatum (including the caudate and putamen), which was defined anatomically based on a normalized T1 image.

Procedures of performance-based regression analysis. The time courses of reward prediction $V(t)$ and reward prediction error $\delta(t)$ were estimated from each subject's performance data—state $s(t)$, action $a(t)$ and reward $r(t)$—as described below.

Reward prediction. To estimate how much of a forthcoming reward a subject would have expected at each step during the Markov decision task, we took the definition of the value function (equation 1) and reformulated it based on the recursive structure of the task. Namely, if the subject starts from a state $s(t)$ and comes back to the same state after k steps, the expected cumulative reward $V(t)$ should satisfy the consistency condition $V(t) = r(t+1) + \gamma\, r(t+2) + \ldots + \gamma^{k-1} r(t+k) + \gamma^k V(t)$.

Thus, for each time t of the data file, we calculated the weighted sum of the rewards acquired until the subject returned to the same state and estimated the value function for that episode as

$$\hat{V}(t) = \frac{\left[r(t+1) + \gamma r(t+2) + \Lambda + \gamma^{k-1} r(t+k) \right]}{1-\gamma^k} \qquad (1)$$

The estimate of the value function $V(t)$ at time t was given by the average of all previous episodes from the same state as at time t

$$V(t) = \frac{1}{L} \sum_{l=1}^{L} \hat{V}(t_l) \qquad (2)$$

where $\{t_1, \ldots, t_L\}$ are the indices of time visiting the same state as $s(t)$, that is, $s(t_1) = \ldots = s(t_L) = s(t)$.

Reward prediction error. The TD error (equation 2) was calculated from the difference between the actual reward $r(t)$ and the temporal difference of the estimated value function $V(t)$.

We separately calculated the time courses of $V(t)$ and $\delta(t)$ during SHORT and LONG conditions; we concatenated data of four blocks in the SHORT condition, and calculated $V(t)$ and $\delta(t)$ as described above. We used the same process for the LONG condition data. During the NO and RANDOM conditions, the values of $V(t)$ and $\delta(t)$ were fixed at zero. Finally, we reconstructed the data corresponding to the real time course of the experiment. Examples of the time course of these variables are shown in **Supplementary Figure 1** online. We used either $V(t)$ or $\delta(t)$ as the explanatory variable in a regression analysis by SPM. To remove any effects of factors other than reward prediction, we concurrently used other variables in the regression, namely the four box-car functions representing each condition (NO, SHORT, RANDOM, LONG). Because the immediate reward prediction $V(t)$ with $\gamma = 0$ can coincide with reward outcome $r(t)$ if learning is perfect, we included the reward outcome $r(t)$ in regression analyses with $V(t)$. Thus, the significant correlation with $V(t)$ (**Fig. 6a,b**) should represent a predictive component rather than a reward outcome.

The amplitude of explanatory variables $\delta(t)$ with all γ were large in early trials and decreased as subjects learned the task (**Supplementary Fig. 1** online). This decreasing trend causes a risk that areas that are activated early in trials, such as those responsible for general attentiveness or novelty, have correlations with $\delta(t)$. Because our aim in regression analysis was to clarify the brain structures involved in reward prediction at specific time scales, we removed the areas that had similar correlation to $\delta(t)$ at all settings of γ from considerations in **Figure 6** and **Supplementary Table 3** online. To compare the results of regression analysis

with six different values of γ, we used display software that can overlay multiple activation maps in different colors on a single brain structure image. When a voxel is significantly activated in multiple values of γ, it is shown by a mosaic of multiple colors, with apparent subdivision of the voxel (Fig. 6).

Note: Supplementary information is available on the Nature Neuroscience website.

ACKNOWLEDGMENTS

We thank K. Samejima, N. Schweighofer, M. Haruno, H. Imamizu, S. Higuchi, T. Yoshioka, T. Chaminade and M. Kawato for helpful discussions and technical advice. This research was funded by 'Creating the Brain,' Core Research for Evolutional Science and Technology (CREST), Japan Science and Technology Agency.

COMPETING INTERESTS STATEMENT

The authors declare that they have no competing financial interests.

Received 5 March; accepted 2 June 2004
Published online at http://www.nature.com/natureneuroscience/

1. Bechara, A., Damasio, H. & Damasio, A.R. Emotion, decision making and the orbitofrontal cortex. *Cereb. Cortex* **10**, 295–307 (2000).
2. Mobini, S. *et al.* Effects of lesions of the orbitofrontal cortex on sensitivity to delayed and probabilistic reinforcement. *Psychopharmacology (Berl.)* **160**, 290–298 (2002).
3. Cardinal, R.N., Pennicott, D.R., Sugathapala, C.L., Robbins, T.W. & Everitt, B.J. Impulsive choice induced in rats by lesions of the nucleus accumbens core. *Science* **292**, 2499–2501 (2001).
4. Rogers, R.D. *et al.* Dissociable deficits in the decision-making cognition of chronic amphetamine abusers, opiate abusers, patients with focal damage to prefrontal cortex, and tryptophan-depleted normal volunteers: evidence for monoaminergic mechanisms. *Neuropsychopharmacology* **20**, 322–339 (1999).
5. Evenden, J.L. & Ryan, C.N. The pharmacology of impulsive behaviour in rats: the effects of drugs on response choice with varying delays of reinforcement. *Psychopharmacology (Berl.)* **128**, 161–170 (1996).
6. Mobini, S., Chiang, T.J., Ho, M.Y., Bradshaw, C.M. & Szabadi, E. Effects of central 5-hydroxytryptamine depletion on sensitivity to delayed and probabilistic reinforcement. *Psychopharmacology (Berl.)* **152**, 390–397 (2000).
7. Doya, K. Metalearning and neuromodulation. *Neural Net.* **15**, 495–506 (2002).
8. Berns, G.S., McClure, S.M., Pagnoni, G. & Montague, P.R. Predictability modulates human brain response to reward. *J. Neurosci.* **21**, 2793–2798 (2001).
9. Breiter, H.C., Aharon, I., Kahneman, D., Dale, A. & Shizgal, P. Functional imaging of neural responses to expectancy and experience of monetary gains and losses. *Neuron* **30**, 619–639 (2001).
10. O'Doherty, J.P., Deichmann, R., Critchley, H.D. & Dolan, R.J. Neural responses during anticipation of a primary taste reward. *Neuron* **33**, 815–826 (2002).
11. O'Doherty, J.P., Dayan, P., Friston, K., Critchley, H. & Dolan, R.J. Temporal difference models and reward-related learning in the human brain. *Neuron* **38**, 329–337 (2003).
12. Sutton, R.S. & Barto, A.G. *Reinforcement Learning* (MIT Press, Cambridge, Massachusetts, 1998).
13. Houk, J.C., Adams, J.L. & Barto, A.G. in *Models of Information Processing in the Basal Ganglia* (eds. Houk, J.C., Davis, J.L. & Beiser, D.G.) 249–270 (MIT Press, Cambridge, Massachusetts, 1995).
14. Schultz, W., Dayan, P. & Montague, P.R. A neural substrate of prediction and reward. *Science* **275**, 1593–1599 (1997).
15. Doya, K. Complementary roles of basal ganglia and cerebellum in learning and motor control. *Curr. Opin. Neurobiol.* **10**, 732–739 (2000).
16. McClure, S.M., Berns, G.S. & Montague, P.R. Temporal prediction errors in a passive learning task activate human striatum. *Neuron* **38**, 339–346 (2003).
17. Mesulam, M.M. & Mufson, E.J. Insula of the old world monkey. III: Efferent cortical output and comments on function. *J. Comp. Neurol.* **212**, 38–52 (1982).
18. Cavada, C., Company, T., Tejedor, J., Cruz-Rizzolo, R.J. & Reinoso-Suarez, F. The anatomical connections of the macaque monkey orbitofrontal cortex. *Cereb. Cortex* **10**, 220–242 (2000).
19. Chikama, M., McFarland, N.R., Amaral, D.G. & Haber, S.N. Insular cortical projections to functional regions of the striatum correlate with cortical cytoarchitectonic organization in the primate. *J. Neurosci.* **17**, 9686–9705 (1997).
20. Balleine, B.W. & Dickinson, A. The effect of lesions of the insular cortex on instrumental conditioning: evidence for a role in incentive memory. *J. Neurosci.* **20**, 8954–8964 (2000).
21. Knutson, B., Fong, G.W., Bennett, S.M., Adams, C.M. & Hommer, D. A region of mesial prefrontal cortex tracks monetarily rewarding outcomes: characterization with rapid event-related fMRI. *Neuroimage* **18**, 263–272 (2003).
22. Ullsperger, M. & von Cramon, D.Y. Error monitoring using external feedback: specific roles of the habenular complex, the reward system, and the cingulate motor area revealed by functional magnetic resonance imaging. *J. Neurosci.* **23**, 4308–4314 (2003).
23. O'Doherty, J., Critchley, H., Deichmann, R. & Dolan, R.J. Dissociating valence of outcome from behavioral control in human orbital and ventral prefrontal cortices. *J. Neurosci.* **23**, 7931–7939 (2003).
24. Koepp, M.J. *et al.* Evidence for striatal dopamine release during a video game. *Nature* **393**, 266–268 (1998).
25. Elliott, R., Friston, K.J. & Dolan, R.J. Dissociable neural responses in human reward systems. *J. Neurosci.* **20**, 6159–6165 (2000).
26. Knutson, B., Adams, C.M., Fong, G.W. & Hommer, D. Anticipation of increasing monetary reward selectively recruits nucleus accumbens. *J. Neurosci.* **21**, RC159 (2001).
27. Pagnoni, G., Zink, C.F., Montague, P.R. & Berns, G.S. Activity in human ventral striatum locked to errors of reward prediction. *Nat. Neurosci.* **5**, 97–98 (2002).
28. Elliott, R., Newman, J.L., Longe, O.A. & Deakin, J.F. Differential response patterns in the striatum and orbitofrontal cortex to financial reward in humans: a parametric functional magnetic resonance imaging study. *J. Neurosci.* **23**, 303–307 (2003).
29. Haruno, M. *et al.* A neural correlate of reward-based behavioral learning in caudate nucleus: a functional magnetic resonance imaging study of a stochastic decision task. *J. Neurosci.* **24**, 1660–1665 (2004).
30. Reynolds, J.N. & Wickens, J.R. Dopamine-dependent plasticity of corticostriatal synapses. *Neural Net.* **15**, 507–521 (2002).
31. Tremblay, L. & Schultz, W. Reward-related neuronal activity during go-nogo task performance in primate orbitofrontal cortex. *J. Neurophysiol.* **83**, 1864–1876 (2000).
32. Critchley, H.D., Mathias, C.J. & Dolan, R.J. Neural activity in the human brain relating to uncertainty and arousal during anticipation. *Neuron* **29**, 537–545 (2001).
33. Rogers, R.D. *et al.* Choosing between small, likely rewards and large, unlikely rewards activates inferior and orbital prefrontal cortex. *J. Neurosci.* **19**, 9029–9038 (1999).
34. Rolls, E.T. The orbitofrontal cortex and reward. *Cereb. Cortex* **10**, 284–294 (2000).
35. Hanakawa, T. *et al.* The role of rostral Brodmann area 6 in mental-operation tasks: an integrative neuroimaging approach. *Cereb. Cortex* **12**, 1157–1170 (2002).
36. Owen, A.M., Doyon, J., Petrides, M. & Evans, A.C. Planning and spatial working memory: a positron emission tomography study in humans. *Eur. J. Neurosci.* **8**, 353–364 (1996).
37. Baker, S.C. *et al.* Neural systems engaged by planning: a PET study of the Tower of London task. *Neuropsychologia* **34**, 515–526 (1996).
38. Middleton, F.A. & Strick, P.L. Basal ganglia and cerebellar loops: motor and cognitive circuits. *Brain Res. Brain Res. Rev.* **31**, 236–250 (2000).
39. Haber, S.N., Kunishio, K., Mizobuchi, M. & Lynd-Balta, E. The orbital and medial prefrontal circuit through the primate basal ganglia. *J. Neurosci.* **15**, 4851–4867 (1995).
40. Eagle, D.M., Humby, T., Dunnett, S.B. & Robbins, T.W. Effects of regional striatal lesions on motor, motivational, and executive aspects of progressive-ratio performance in rats. *Behav. Neurosci.* **113**, 718–731 (1999).
41. Pears, A., Parkinson, J.A., Hopewell, L., Everitt, B.J. & Roberts, A.C. Lesions of the orbitofrontal but not medial prefrontal cortex disrupt conditioned reinforcement in primates. *J. Neurosci.* **23**, 11189–11201 (2003).
42. Hikosaka, O. *et al.* Parallel neural networks for learning sequential procedures. *Trends Neurosci.* **22**, 464–471 (1999).
43. Mijnster, M.J. *et al.* Regional and cellular distribution of serotonin 5-hydroxytryptamine2a receptor mRNA in the nucleus accumbens, olfactory tubercle, and caudate putamen of the rat. *J. Comp. Neurol.* **389**, 1–11 (1997).
44. Compan, V., Segu, L., Buhot, M.C. & Daszuta, A. Selective increases in serotonin 5-HT1B/1D and 5-HT2A/2C binding sites in adult rat basal ganglia following lesions of serotonergic neurons. *Brain Res.* **793**, 103–111 (1998).
45. Celada, P., Puig, M.V., Casanovas, J.M., Guillazo, G. & Artigas, F. Control of dorsal raphe serotonergic neurons by the medial prefrontal cortex: involvement of serotonin-1A, GABA(A), and glutamate receptors. *J. Neurosci.* **21**, 9917–9929 (2001).
46. Martin-Ruiz, R. *et al.* Control of serotonergic function in medial prefrontal cortex by serotonin-2A receptors through a glutamate dependent mechanism. *J. Neurosci.* **21**, 9856–9866 (2001).
47. Hikosaka, K. & Watanabe, M. Delay activity of orbital and lateral prefrontal neurons of the monkey varying with different rewards. *Cereb. Cortex* **10**, 263–271 (2000).
48. Shidara, M. & Richmond, B.J. Anterior cingulate: single neuronal signals related to degree of reward expectancy. *Science* **296**, 1709–1711 (2002).
49. Matsumoto, K., Suzuki, W. & Tanaka, K. Neuronal correlates of goal-based motor selection in the prefrontal cortex. *Science* **301**, 229–232 (2003).

Eur Arch Psychiatry Clin Neurosci (2004) 254 : 245–251 DOI 10.1007/s00406-004-0488-z

ORIGINAL PAPER

Shuji Asahi · Yasumasa Okamoto · Go Okada · Shigeto Yamawaki · Norio Yokota

Negative correlation between right prefrontal activity during response inhibition and impulsiveness: A fMRI study

Received: 5 May 2003 / Accepted: 8 December 2003

Abstract Behavioral disinhibition in Go/No-Go task is thought to be associated with impulsiveness in humans. Recent imaging studies showed that neural circuits involving diverse areas of the frontal cortex and other association cortex sites such as the parietal cortex are implicated in the inhibition of response during No-Go trials. The aim of the present study was to investigate the association between regional cerebral activation during No-Go trials and impulsiveness. Seventeen right-handed healthy volunteers participated in the study. We used functional magnetic resonance imaging to measure the brain activation during a Go/No-Go task. The Barratt Impulsiveness Scale, 11th version (BIS-11) was used to measure impulsiveness. Activated regions included the right middle frontal gyrus and the inferior parietal lobe, which is consistent with previous neuroimaging studies. A negative correlation was observed between the motor impulsiveness of BIS-11 and No-Go-related activation in the right dorsolateral prefrontal cortex (RDLPFC). Our results suggest that the RDLPFC is the area most sensitive to differences in individual motor impulsiveness and its activity may be an indicator of the individual capacity for response inhibition.

Key words response inhibition · fMRI · right dorsolateral prefrontal cortex (RDLPFC) · impulsiveness · BIS

Sh. Asahi · Y. Okamoto · G. Okada · Sh. Yamawaki, M.D., Ph.D. (✉)
Department of Psychiatry and Neurosciences
Graduate School of Biomedical Sciences
Hiroshima University
1-2-3 Kasumi, Minami-ku
Hiroshima, 734-8551, Japan
Tel.: +81-82/257-5205
Fax: +81-82/257-5209
E-Mail: yamawaki@hiroshima-u.ac.jp

N. Yokota
Hiroshima Prefectural College of Health and Welfare
Hiroshima, 723-0053, Japan

Introduction

Impulsiveness is a dimensional personality trait that is important for a wide range of different human behaviors. Although a strict definition of impulsiveness is difficult to establish, biological, psychological and social studies have regarded impulsiveness as 'a predisposition toward rapid, unplanned reactions to internal or external stimuli without regard to the negative consequences of these reactions to the impulsive individual or to others' [34]. Recent laboratory investigations of impulsiveness showed two dominant models: (1) *Reward-delay impulsivity*, which is the inability to delay reward and leads to an increased tendency to choose immediate small rewards over larger delayed ones [35]; and (2) *Rapid-response impulsivity*, which is the inability to conform responses to environmental context and leads to errors of commission on tests that require careful checking of stimuli [16]. The latter model appeared to be more closely related to trait impulsiveness, which was measured by the Barratt Impulsiveness Scale (BIS), a popular self-reporting impulsiveness scale [37], and was increased in subjects with a lifetime Axis I or Axis II diagnosis [49].

The ability to inhibit behavioral responses that are inappropriate in the current context is a response inhibition essential for normal behavior, and is thought to be associated with *Rapid-response impulsivity* in humans. This inhibitory function has been investigated frequently using the Go/No-Go task, in which the participants are required to refrain from responding to designated items within a series of stimuli. The prefrontal cortex (PFC) has been implicated in behavioral inhibition, based on animal, clinical and neuroimaging studies. Studies in monkeys demonstrated that lesions in the PFC resulted in difficulties in behavioral inhibition [8, 24, 45], as well as the studies of patients with lesions in the same region [22]. Recent neuroimaging studies using PET or fMRI have shown a right hemispheric dominance of inhibitory control that involves diverse areas of

the frontal cortex and other association cortex sites, such as the parietal cortex, which are implicated in response inhibition during No-Go trials [21, 26, 30]. Although human impulsiveness was revealed to associate with some biological markers [1, 17, 42, 50], the region of the brain that is directly correlated with human impulsiveness is still unclear.

Some experiments used only behavioral laboratory measurements of impulsiveness [11, 21], which do not incorporate the cognitive or social aspects of impulsiveness and do not measure long-term patterns of behavior. This may explain the inconsistency in the findings of those previous studies [9, 33, 38]. Another way to examine impulsiveness is to use self-reporting measurements such as BIS, which has the advantage of generating information on a variety of types of acts and on whether these acts continue as long-term patterns of behavior. In general, a closer association and a greater consistency has been demonstrated among different self-report impulsiveness scales [3, 9, 15].

The aim of the present study was to clarify the brain areas associated with impulsiveness, as measured by BIS-11. Based on the studies cited above, we hypothesized that the degree of activation in some areas within the right hemispheric dominance of neural networks was correlated with the degree of impulsiveness.

Methods

Subjects

Seventeen right-handed healthy volunteers (10 men and 7 women), aged 23–30 years (mean: 25.1 years), and with no history of neurological or psychiatric illness, participated in the study. Handedness was assessed by the Edinburgh Handedness Inventory [36]. The subjects were recruited from the Kansai area in Japan and were paid ¥7,000 for their participation in the study. The study was conducted under a protocol that was approved by the Ethics Committee of Hiroshima University School of Medicine. All subjects submitted informed written consent of their participation.

Barratt Impulsiveness Scale, 11th version

The BIS-11 [37], a short questionnaire designed to measure impulsiveness, has been validated in impulsive and normal populations. The questionnaire contains a total of 30 items, each of which is answered on a 4-point Likert scale (rarely/never = 1, occasionally = 2, often = 3, almost always/always = 4), and the level of impulsiveness is calculated by summing up the scores for each item. All items are defined as identifying impulsiveness within the structure of related personality traits and are divided into three subscales: attention (inattention and cognitive instability), motor (motor impulsiveness and lack of perseverance), and non-planning (lack of self-control and intolerance of cognitive complexity). The Japanese version of the BIS-11 was developed using a back-translation method and was judged to be a reliable and valid measure in the Japanese population [47]. Subjects completed the BIS-11 after the task procedure.

Experimental tasks

The task consisted of eight alternating 36-s epochs of Go and No-Go conditions. During the experiment, subjects viewed a series of letters once every 1500 ms and responded with a key press to every letter except the letter 'X', to which they were instructed to withhold response. All subjects responded using the forefinger of the right hand. Stimulus duration was 500 ms and the interstimulus interval was 1000 ms for both conditions. Subjects were instructed to try to respond while the stimulus was on the screen. In the Go (control) condition, subjects were presented a random sequence of letters other than the letter 'X'. In the No-Go condition, subjects were presented with the letter 'X' 50% of the time, thus requiring a response to half the trials (Go trials) and a response inhibition to the other half (No-Go trials). The high frequency of targets was maintained across the entire experiment, which generated a compelling tendency to respond. In order to ensure correct performance, the subjects were trained outside the task scanner until they understood the task completely. Motor responses were made using a fiber-optic response pad (Current Designs Inc, Philadelphia). The task consisted of eight blocks, each of which continues without being preceded by an instruction. The subjects could not distinguish the boundary between the conditions; therefore, different strategies are not imposed on the subject for the different conditions.

fMRI acquisition

Functional magnetic resonance imaging (fMRI) was performed using a Magnex Eclipse 1.5T Power Drive 250 (Marconi Medical Systems, USA). A time-course series of 107 volumes was acquired with T2*-weighted, gradient echo, echo planar imaging (EPI) sequences. Each volume consisted of 38 slices, and the slice thickness was 4.0 mm with no gap to cover the entire cerebral and cerebella cortex. The interval between two successive acquisitions of the same image (TR) was 4000 ms, echo time (TE) was 55 ms, and the flip angle was 90°. The field of view was 256 mm, and the matrix size was 64 × 64, giving voxel dimensions of 4.0 × 4.0 × 4.0 mm. After functional scanning, structural scans were acquired using Tl-weighted gradient echo pulse sequence (TR = 12 ms; TE = 4.5 ms; Flip angle = 20°; FOV = 256 mm; voxel dimensions of 1.0 × 1.0 × 1.0 mm), which facilitated the localization and coregistration of functional data.

Analysis

The image data were analyzed by statistical parametric mapping (SPM99 software from the Wellcome Department of Cognitive Neurology, London, UK) implemented in Matlab (Mathworks Inc., Sherborn, MA). The first three volumes of each fMRI run (prescan period) were discarded because the magnetization was unsteady. The remaining 104 volumes were used for the statistical analysis. Images were corrected for motion and realigned, using the first scan of the session as a reference. T1 anatomical images were coregistered to the first functional scans and aligned to the T1 template included in SPM99. The calculated nonlinear transformation was applied to all functional images for spatial normalization. Finally, the functional images were smoothed with an 8 mm full-width, half-maximum (FWHM) Gaussian filter. Using group analysis according to a random effect model [18], we identified regions that showed significant responses to the No-Go condition compared with that of the Go condition as areas related to response inhibition. The group analysis consisted of two levels. In the first level, the signal time course of each subject was modeled with a delayed box-car function convolved with a hemodynamic response function in the context of a general linear model. One contrast image per subject was created by contrasting the No-Go conditions with the Go conditions. These images were entered into a one-sample t-test, which allowed us to identify regions of the brain that were significantly activated by the response inhibition function during the No-Go condition as compared to the Go condition. The resulting foci were then characterized in terms of spatial extent (k) and peak height (u). The significance of each region was estimated using distribution approximations from the theory of Gaussian fields. This characterization is in terms of the probability that a region of the observed number of voxels (or greater) could have occurred by chance (extent threshold) over the entire volume analyzed. After locating and analyzing areas of the brain that showed sig-

nificant activation during the No-Go condition, we then performed a regression analysis on these areas only, to determine the association between the magnitude of brain activation in each area and the scores of the BIS-11. Activations were reported if they exceeded $p < 0.001$ (uncorrected) on the single voxel level and $p < 0.05$ (corrected) on the cluster level. In regression analysis, we masked with the regions that showed significant responses to the No-Go condition compared with that of the Go condition, as the areas related to response inhibition described above, to avoid identifying regions that were not activated for the No-Go condition compared with the Go condition. However, when using a lower threshold, an activation that was at a lower level but consistent with the significant activation noted above was seen over more widespread areas of the brain. This occurred because the threshold for this mask was set at $p < 0.05$ and larger areas are included in the final analysis of the response inhibition data. Therefore, significance was considered at a threshold of $p < 0.001$ and an extent of > 40 contiguous voxels. Labels for brain activation foci were obtained in Talairach coordinates using the Talairach Demon software, which provides an accuracy similar to that of neuroanatomical experts [28].

Behavioral analysis

Errors of commission (response to 'X') and omission (not to response to targets) were recorded, and the average response times to targets were calculated for each subject.

Results

Behavioral and BIS-11 results

Subjects performed well on the task, making a few commission errors (7.3 %) and a few omission errors (1.3 %). The response times to targets averaged 325.8 ± 20.8 ms. Average scores of the total BIS-11, attention-key, motor-key and non-planning-key were 68.9 ± 11.0, 19.7 ± 3.3, 21.1 ± 4.1 and 28.1 ± 5.3, respectively. Some correlation was detected among the BIS-11 scales. The total score of BIS-11 was strongly correlated with all of the 3 subscales (attention-key: $r = 0.69$, $p < 0.01$; motor-key: $r = 0.89$, $p < 0.01$; non-planning-key: $r = 0.93$, $p < 0.01$). Among the subscales, the non-planning-key and attention-key ($r = 0.51$, $p < 0.05$), or non-planning-key and motor-key ($r = 0.79$, $p < 0.01$) were correlated. There was also a trend between attention-key and motor-key, though not significant ($r = 0.48$, $p = 0.05$). These results were natural because the BIS-11 has sufficient internal consistency reliability [47]. No correlation was observed between the performance data (i. e., number of commission errors or omission errors, average response time to targets) and the BIS-11 scores.

fMRI data

For fMRI data analysis, the threshold for activation was set at $p < 0.001$ for voxel level. In Fig. 1 and Table 1, the activation, which was corrected for multiple comparisons at the extent threshold of $p < 0.05$, is shown. Four independent areas of activation, which were predominantly right-lateralized, were observed to underlie response inhibition. These areas, including the Talairach coordinates of their centers-of-mass, are presented in Table 1. The No-Go condition, in comparison to the Go condition, resulted in the significant activation of the right middle and superior temporal gyrus, the right precentral gyrus, the right middle frontal gyrus, and the right cuneus and precuneus.

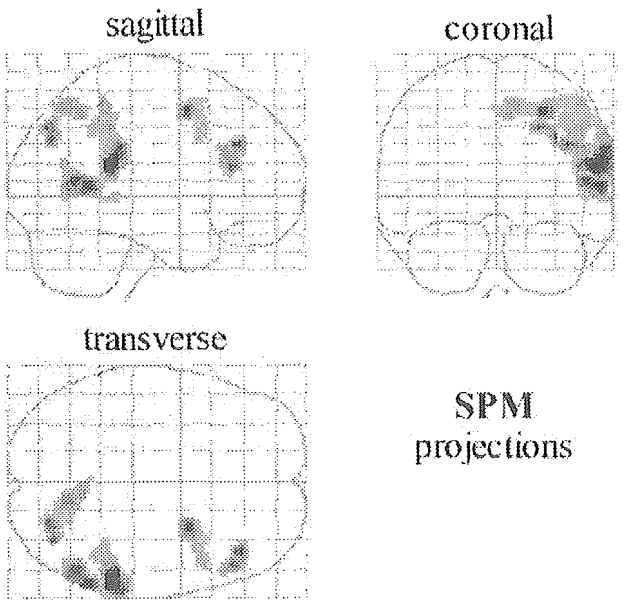

Fig. 1 Statistical parametric maps of brain regions (on the second level group analysis for the 17 subjects) showing significant activation associated with the NO-GO condition, compared with the GO condition at a statistical threshold of $P < 0.001$ (uncorrected) on the single voxel level and $P < 0.05$ (corrected) on the cluster level. For exact coordinates, see Table1. Clusters of activation are shown as through-projections onto representations of standard stereotactic space. *Sagittal* side view; *coronal* view from back; *transverse* view from above

Regression analysis revealed a significant negative correlation between the motor-key score of BIS-11 and the magnitude of brain activation during response inhibition in the right middle frontal gyrus (x, y, z = 34, 22, 29; area 9; t-value = 5.66; 42 voxels; $r = -0.93$; $p < 0.01$) showed in Fig. 2A, B. Other BIS-11 scores (i. e., total BIS-11, attention-key and non-planning-key) did not show a significant association with the magnitude of brain activation during response inhibition. Furthermore, no significant correlation was observed between the performance data (i. e., the number of commission errors and omission errors, response time) and the magnitude of brain activation during response inhibition.

By analyzing the mean percentage signal changes in the regions shown in Fig. 1 and Table 1, we sought to find the possible functional connectivity among the regions concerning response inhibition. Consequently, we detected a correlation between the areas including the right middle frontal/the right precentral gyrus and the right cuneus/precuneus ($r = 0.65$, $p < 0.01$). There was no correlation between the other regions.